Kinetic Studies, Mechanism, and Substrate Specificity of Amadoriase I from *Aspergillus sp.*†

Xinle Wu,‡ Bruce A. Palfey,*,§ Valeri V. Mossine,|| and Vincent M. Monnier*,‡

Institute of Pathology, Case Western Reserve University, Cleveland, Ohio 44106, and Department of Biological Chemistry, University of Michigan Medical School, Ann Arbor, Michigan 48109, and Department of Biochemistry, University of Missouri, Columbia, Missouri 65211

Received June 15, 2001; Revised Manuscript Received August 27, 2001

ABSTRACT: Amadoriase is a flavoenzyme that catalyzes the oxidative deglycation of Amadori products (fructosyl amino acids or aliphatic amines) to yield free amine, glucosone, and hydrogen peroxide. The mechanism of action of amadoriase I from *Aspergillus sp.* has been investigated by stopped-flow kinetic studies using fructosyl propylamine and O_2 as substrates in 10 mM Tris HCl, pH 7.9, 4 °C. Using both substrate analogues and fast kinetic techniques, the active configuration of the substrate was found to be the β-pyranose form. Stopped-flow studies showed that the reductive half-reaction is triphasic and generates intermediates that absorb at long wavelengths and is consistent either with (i) the reaction of the substrate with the flavin followed by iminium deprotonation or hydrolysis and then product release or with (ii) the formation of flavin reduction intermediates (carbanion equivalents or adducts), followed by product release. The rate of product release after flavin reduction is lower than the aerobic turnover rate, 14.4 s^{-1}, suggesting that it is not involved in the catalytic cycle and that reoxidation of the reduced enzyme occurs in the E_{red}−product complex. In the oxidative half-reaction, the reduced flavin is oxidized by O_2 in a single phase. The observed rate constant has a linear dependence on oxygen concentration, giving a bimolecular rate constant of 4.9×10^4 M^{-1} s^{-1} in the absence of product, and 3.6×10^4 M^{-1} s^{-1} when the product is bound. The redox potentials of amadoriase have been measured at pH 7.0, 25°, giving values of +48 and −52 mV for the oxidized enzyme/anionic semiquinone and anionic semiquinone/reduced enzyme couples, respectively.

Amadoriase is a flavoprotein that catalyzes the oxidation of Amadori products by oxygen to yield glucosone, an amine and hydrogen peroxide (*1*).

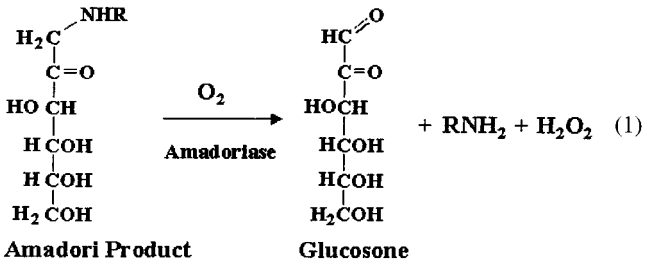

(1)

The Amadori product is the initial product of the Maillard glycation reaction of proteins, produced when glucose reacts nonenzymatically with amino groups in proteins to form ketoamino-linked 1-deoxyfructosyl adducts. It is the precursor of protein cross-links and glycoxidation products that accumulate in long-lived proteins (*2*−*4*) and has been implicated in the development of diabetic complications and the aging process (*5*−*8*). Previously, we reported the isolation and cloning of two amadoriase isoenzymes from *Aspergillus sp.* from soil which we named amadoriase I and II (1). These enzymes are monomers of molecular mass around 40−50 kDa containing FAD as the cofactor. Amadoriase I has one FAD covalently bound to cysteine 342 (*9*).

Amadoriase catalyzes the FAD-dependent reaction of O_2 and Amadori products to the corresponding imine and hydrogen peroxide. In this paper, we address the mechanism of the amadoriase I by employing stopped-flow spectrophotometry and [$^1H_2$]- and [$^2H_2$]-fructosyl *n*-propylamine (PAAP)[1] as substrate. Steady-state kinetics, the reductive half-reaction, and the oxidative half-reaction have been analyzed. We propose a minimal kinetic scheme for this enzyme that involves a charge-transfer intermediate (*10*). We also identified the substrate configuration recognized by the enzyme.

EXPERIMENTAL PROCEDURES

Materials. 2,5-Anhydro mannitol, 1,5-anhydro mannitol, fructose, and glucose were purchased from Sigma (St. Louis,

† This work was supported by a grant from the National Eye Institute (EY 07099) and EY11373 (Core Grant), and in part by grant AG18629 from the National Institute on Aging. B.A.P. was supported by NIH grants GM20877 to David P. Ballou and GM11106 to Vincent Massey.

* To whom correspondence should be addressed. V.M.M.: Fax: (216) 368-0495. Phone: (216) 368-6613. E-mail: vmm3@po.cwru.edu, B.A.P.: Fax: (603) 687-1852. Phone: (734) 763-2449. E-mail: brupalf@umich.edu.

‡ Case Western Reserve University.

§ University of Michigan Medical School.

|| University of Missouri.

[1] Abbreviations: amadoriase, fructosyl amino acid oxidase (EC 1.5.3); ABTS, 2,2′-azine-bis(3-ethylbenzthiazoline-6-sulfonic acid); HRP, horseradish peroxidase; PAAP, fructosyl *n*-propylamine; NaOD, sodium deuterioxide; DCl, deuterium chloride; NMR, nuclear magnetic resonance; PCA, protocatechuate; PCD, protocatechuate dioxygenase; DTT, dithiothreitol.

10.1021/bi011244e CCC: $20.00
Published on Web 10/06/2001

MO). Hydroxyapatite matrix was from Bio-Rad (Hercules, CA), and Ni-NTA Superflow resin was from Qiagen (Valencia, CA). All the other chemicals were from Sigma. Fructosyl propylamine was synthesized as reported in Takahashi et al. (*1*). Methyl β-fructofuranoside and methyl α-fructofuranoside were prepared according to the published methods (*34*−*36*). In brief, a fructose solution in anhydrous methanol containing 1% TFA was kept for 4 days at room temperature, and then neutralized with anionite (OH^--form). Separation of the methyl fructosides was achieved on a column packed with Bio-Rad AG 1 × 8 resin (OH^--form), with water as eluent.

Enzyme Purification. Expression of recombinant amadoriase I from *Aspergillus sp*. and purification by Ni-NTA Superflow FPLC column (Pharmacia) were performed as described by Wu et al. (*9*). Proteins were dialyzed overnight against 10 mM sodium phosphate buffer (pH 7.4) and applied to a hydroxyapatite column (10 × 10 cm) equilibrated with the same buffer. After the column was washed with 300 mL of equilibration buffer, elution was carried out with a 1000-mL linear gradient of sodium phosphate buffer (pH 7.4), from 10 to 200 mM with a flow rate of 5 mL/min. Fractions with enzyme activity were pooled and concentrated with an Amicon Centriprep using YM-10 membrane (Millipore, Bedford, MA). Proteins were dialyzed against 10 mM Tris HCl buffer (pH 7.4).

Determination of the Extinction Coefficient of Amadoriase. The extinction coefficient was determined by titrating the reduced enzyme with potassium ferricyanide. Enzyme (200 μL) was mixed with 1000 μL of 8 M guanidine hydrochloride and 10 mM EDTA in a glass vessel and was made anaerobic. The enzyme was then fully reduced by strong white light radiation (*27*). Potassium ferricyanide solution with a concentration of approximately 1 mM was bubbled with purified argon and loaded into a syringe for the titration. Spectra were recorded after each 5 μL addition of potassium ferricyanide until the absorbance at 453 nm reached a maximum. The concentration of potassium ferricyanide was determined using its extinction coefficient at 420 nm (1000 M^{-1} cm^{-1}).

Determination of Redox Potentials. The redox potentials of amadoriase were determined at 25 °C using the xanthine/xanthine oxidase reduction system of Massey (*11*). For this, 20−30 μM enzyme in 0.1 M potassium phosphate, pH 7.0, together with 0.2 mM xanthine and an appropriate amount of redox indicator dye were mixed together and made anaerobic in a cuvette. To ensure rapid equilibration of reducing equivalents, 2 μM benzyl viologen was also included. The reaction was started by adding xanthine oxidase (10−50 nM) from the sidearm of the cuvette, and absorbance spectra were collected at various times.

Inhibition Assays. Enzyme activity was determined by the ABTS assay that measures hydrogen peroxide. Reaction mixtures contained 90 μL of 10 mM HEPES, pH 8.0, 30 μL of 10 mg/mL ABTS, and 2 mg/mL peroxidase mixture, 30 μL of purified enzyme solution, and 50 μL of substrate (fructosyl ϵ-amine caproic acid)/inhibitor mixture in a total volume of 200 μL in a 96-well microplate. After 20 min, the absorbance at 415 nm was measured on a microplate reader (model 450, Bio-Rad, CA).

Synthesis of [$^2H_2$]-PAAP. Fructosyl *n*-propylamine (PAAP) was dissolved in D_2O and NaOD was used to adjust the pD to 10.4. After incubating overnight at 25°, protons on C1 of PAAP exchanged with solvent deuterium. The pD was titrated to 8.1 with DCl, and the solution was lyophilized for storage and later dissolved with 10 mM Tris HCl buffer (pH 7.9, 4°) at the desired concentration immediately before use to prevent the back exchange of protons. The structure of [$^2H_2$]-PAAP was confirmed by mass spectroscopy (LCQ, ThermalQuest, FL) and ^{13}C NMR.

Stopped-Flow Kinetics. Rapid reaction measurements and turnover experiments were carried out in a Kinetic Instruments stopped-flow spectrophotometer, a Hi-Tech SF-61 stopped-flow spectrophotometer/fluorimeter, or a Hi-Tech SF-61 DX-2 instrument equipped with a diode-array detector. The spectral acquisition time of the diode array instrument was 1.5 ms. For anaerobic experiments, oxygen was scrubbed from the driving syringes by PCA/PCD (*25*). Enzyme solutions were made anaerobic in tonometers on ice by at least 10 cycles of evacuation followed by filling and equilibrating with purified argon. Substrate solutions were made anaerobic by bubbling with argon for at least 10 minutes. The kinetics of the reductive half-reaction was monitored at 453 and 550 nm after mixing oxidized enzyme with buffer (10 mM Tris HCl, pH 7.4) containing various concentrations of PAAP. The steady-state kinetic analysis was carried out at pH 7.9, 4 °C, using the enzyme monitored turnover method as described by Gibson et al. (*12*).

The oxidation of the reduced enzyme was investigated as follows. The oxidized form of the enzyme was made anaerobic in a tonometer and reduced by adding an equivalent of PAAP. The reduced enzyme was mixed with an equal volume of buffer containing oxygen in the stopped-flow instrument, and the increase in the absorbance at 453 nm was measured. Different oxygen concentrations were obtained by bubbling syringes of buffer with O_2−N_2 mixtures obtained from Matheson. All reactions were carried out at 4 °C.

Analysis of Stopped-Flow Traces. Stopped-flow traces for the reduction and oxidation experiments were analyzed by fitting to the sum of exponentials:

$$A_t = A_{inf} + C_1 \exp(-k_1 t) + C_2 \exp(-k_2 t) + ... + C_n \exp(-k_n t) \quad (2)$$

where A is absorbance, k_i is a (pseudo) first-order rate constant, and C_i is a constant. The program SClamp, a derivative of CLAMP (*24*) from David Myszka, University of Utah, was used for the simultaneous fitting of a series of reaction trace at different PAAP concentrations. Simulations were also performed using Berkeley Madonna 8.0.1.

RESULTS

Extinction Coefficient. Denatured reduced enzyme was titrated with 1.03 mM potassium ferricyanide anaerobically. From the equivalence point, the extinction coefficient of amadoriase was determined as 12 500 M^{-1} cm^{-1} (data not shown).

Redox Potentials. The flavin redox potentials were determined using the method described by Massey (*11*). When the xanthine oxidase-mediated reduction of amadoriase was monitored in the absence of a reference dye, the initial formation of a one-electron-reduced flavin species was

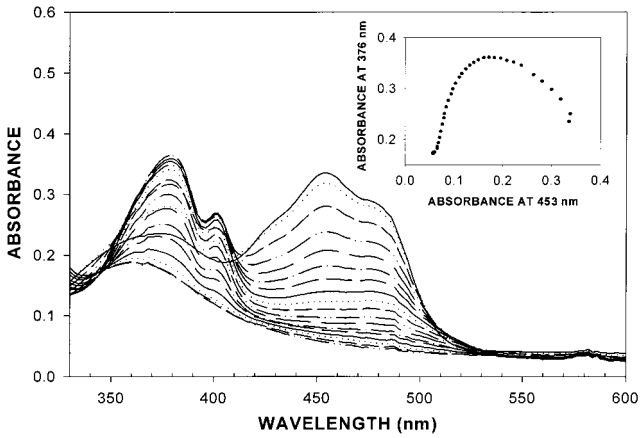

FIGURE 1: Spectral changes during the anaerobic xanthine oxidase-mediated reduction of amadoriase (see Experimental Procedures). Spectra were obtained at regular time intervals (5 min) during the reduction of 27 μM enzyme in 0.1 M phosphate buffer, pH 7.0, at 25°. Inset, absorbance at 453 nm versus the absorbance at 376 nm throughout the experiment.

observed (Figure 1), which had absorbance peaks at 378, 401, and 478 nm, characteristic of anionic (red) flavin semiquinone (*13*). It was estimated that the maximal amount of flavin radical formed during the reduction process was 70% (Figure 1, inset), allowing us to calculate a separation of 80 mV for the redox potentials of the oxidized/semiquinone couple (E_1) and the semiquinone/hydroquinone couple (E_2) (*14*). By using thionin (+60 mV) and indigo tetrasulfonate (−46 mV) as reference dyes, the two redox potentials could be determined separately. The redox potential of the enzyme was calculated by plotting log([ox]/[red]) for the enzyme versus the corresponding log([ox]/[red]) value of the dye (*15*). The two redox potentials E_1 and E_2 were +48 and −52 mV, respectively. These values are in line with the above-mentioned estimated separation of the two redox potentials. Data obtained by reducing the enzyme in the presence of methylene blue (+11 mV) also agreed with these results. The two-electron midpoint redox potential (E_m) of amadoriase is −2 mV [$E_m = (E_1 + E_2)/2$] (*14*).

Reduction by Dithiothreitol. In the early stages of our work, we observed that solutions of Amadoriase would form anionic semiquinone during the process of removing oxygen and prior to the addition of reductants in our experiments. We determined that dithiothreitol (DTT), which we originally included in our buffers, could reduce the enzyme. This was documented by making a solution of amadoriase (21 μM) in 10 mM Tris HCl, pH 7.4, anaerobic in the absence of DTT. No reaction was observed after incubating for an hour at 25°. At this time, an aliquot of a concentrated DTT solution was added from a sidearm of the cuvette to give a final concentration of 1 mM. Anionic semiquinone started to form immediately and reached a maximum level after 2.5 h. The semiquinone was subsequently converted to fully reduced enzyme after ~40 h. Presumably DTT reacts with amadoriase through a two-electron reaction to form the flavin hydroquinone. However, the initial reaction product that was observed was the flavin semiquinone, implying that the reaction between oxidized enzyme (which is initially in large excess) and reduced enzyme is rapid and highly favored. When most of the enzyme is in the semiquinone state, the small amount of oxidized enzyme present will continue to be converted to fully reduced enzyme, pulling the equilibrium to the hydroquinone state at a rate governed by the rate of semiquinone disproportionation.

Table 1: Apparent Steady State Kinetic Parameters for the Reaction of Amadoriase[a]

substrate	k_{cat} (s-1)	$K_m(O_2)$ mM	k_{cat}/K_m mM/s
[$^1H_2$]-PAAP	14.4	1.05	13.7
[$^2H_2$]-PAAP	5.0	0.39	12.9
isotope effect ($^1H/^2H$)	2.9	2.7	1.06

[a] All experiments were performed at pH 7.9, 4 °C. [O_2] = 1.95 mM, [PAAP] = 5 mM (after mixing).

Enzyme-Monitored Turnover. Steady-state kinetic parameters were determined by monitoring the enzyme absorbance during turnover (*12*). Oxidized enzyme (~15 μM final concentration) that had been equilibrated under an atmosphere of 100% O_2 on ice was mixed with 5 mM substrate (PAAP), also equilibrated on ice under an atmosphere of 100% O_2, giving an O_2 concentration of 1.95 mM immediately after mixing in the stop-flow instrument at 4 °C. At 453 nm, a rapid decrease of oxidized flavin absorption was followed by a steady-state phase and then by a further decrease to reach the final reduced state after oxygen was consumed. The analysis of these traces was done according to the method of Gibson et al (*12*). Table 1 lists the corresponding steady-state coefficients for [$^1H_2$]- and [$^2H_2$]-PAAP, respectively. Because the concentration of PAAP that was used (5 mM) was much higher than the K_m of PAAP (0.049 mM) (*9*), the apparent k_{cat} (14.4 s^{-1}) represents the turnover number extrapolated to infinite substrate concentration. An isotope effect of 2.9 was observed on k_{cat}.

Reductive Half-Reaction. When amadoriase and PAAP were mixed in the stopped-flow spectrophotometer under anaerobic conditions at 4°, pH 7.9, three reaction phases were observed at 453 nm (Figure 2). A large decrease in absorbance was observed in the first reaction phase, suggesting that the flavin might be reduced in this reaction. The observed rate constant for the first phase increased to a limiting value of 652 s^{-1} at high PAAP concentrations, and a nonzero intercept of 58 s^{-1} was evident as the concentration of PAAP approached zero (Figure 3). The nonzero intercept indicates that this reaction is reversible, while the saturating PAAP concentration dependence indicates that the reaction responsible for the absorbance change being monitored is preceded by the binding of PAAP. A half-saturating total PAAP concentration of 1.77 mM was obtained. The second reaction phase had about one-third of the amplitude of the first phase, and its observed rate constant increased with PAAP concentration in a hyperbolic fashion, reaching a limiting value of about 25 s^{-1}. The value of the observed rate constant of the third phase decreased slightly as PAAP concentration increased, to a limiting minimum value at 3.5 s^{-1}. A decreasing concentration dependence suggests that a unimolecular step precedes a concentration-dependent event and becomes rate-determining at high PAAP concentrations (*30*). In the present case, the slow reaction represents the dissociation of the product from the reduced enzyme, which is followed by the trapping of the free reduced enzyme by the large excess of unreacted PAAP. Thus, the value of 3.5 s^{-1} represents the rate constant for product dissociation from the reduced enzyme; this value is too small to be catalytically relevant, and we conclude that free reduced enzyme is not a

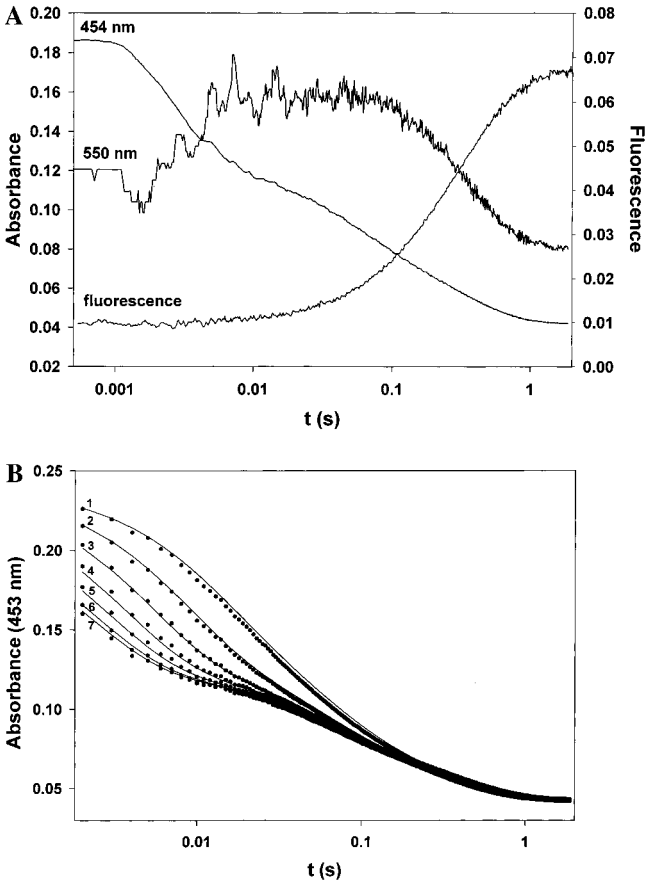

FIGURE 2: (A) Time course of anaerobic reduction of amadoriase, followed by a stopped-flow instrument. 5 mM [$^1H_2$]-PAAP was mixed with 20 μM amadoriase. The experiments were performed in 10 mM Tris HCl buffer, pH 7.9, at 4 °C, and the reported concentrations are the values after mixing. The same concentrations and conditions were used to collect the fluorescence trace (excitation at 350 nm, emission above 500 nm). The 550 nm trace has been multiplied by 10 to facilitate comparison. Note the logarithmic time scale. (B) Simulated reaction traces. Reaction traces using [$^1H_2$]-PAAP are shown overlayed with traces from numerical simulations using the rate constants listed in Table 2. PAAP concentrations for curves 1−7 are 0.125, 0.25, 0.5, 1, 2, 5, and 12.5 mM. Concentrations are for total PAAP, not reactive isomer. Note the logarithmic time scale.

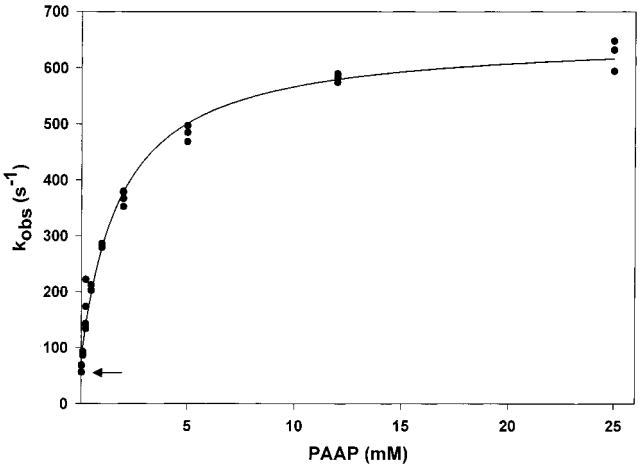

FIGURE 3: Observed rate constant for the first phase in the reduction of amadoriase with varying concentrations of [$^1H_2$]-PAAP. The anaerobic reduction experiments were performed in 10 mM Tris HCl buffer, pH 7.9, at 4 °C. Reaction of the flavin was monitored at 453 nm. Each point on the plot is one mixing experiment. Concentrations are for total PAAP, not reactive isomer. The arrow indicates the value found for the reverse reduction rate.

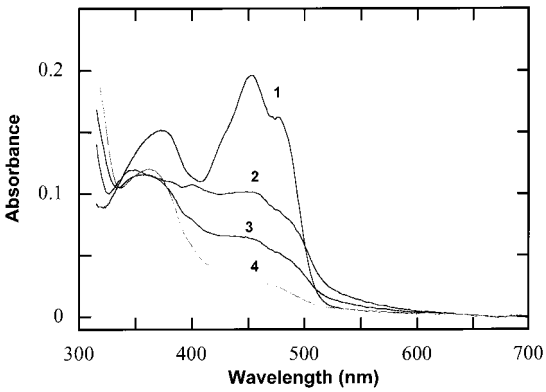

FIGURE 4: Absorption spectra of amadoriase during the reductive half-reaction. Spectral deconvolution was based on the simulation according to eq 3 of the diode-array spectra obtained from the anaerobic reaction of amadoriase and PAAP as substrate in 10 mM Tris HCl buffer, pH 7.9, at 4 °C. 1, E_{ox}∼S; 2, E_{red}∼I; 3, E_{red}∼P; 4, E_{red}∼S.

catalytic intermediate. We also followed the reduction at 550 nm (Figure 2A) and observed the formation and decay of intermediates that absorb at long wavelengths. The rate constants for the changes in absorbance at 550 nm agreed with those obtained at 453 nm, although they were less reliable due to the smaller amplitudes. Absorbance in this spectral region could indicate either a charge-transfer interaction between the reduced flavin and the product (*17*, *18*), or the presence of a neutral (blue) flavin semiquinone. However, traces obtained at 600 nm and longer wavelengths showed no absorbance changes, ruling out the presence of neutral semiquinone. The reductive half-reaction was also investigated using a diode-array detector (Figure 4). Spectral features that are characteristic of flavin semiquinone were not observed.

The same reaction was observed in a stopped-flow instrument using fluorescence detection to observe changes in flavin fluorescence during the reaction. Interestingly, there was no appreciable change until the fluorescence started to increase after ∼60 ms (Figure 2A). The fluorescence increased with an observed rate constant of 3.1 s^{-1}, essentially the same value obtained for product dissociation. Thus, we found that the reduced enzyme is more fluorescent than the oxidized enzyme or any of the reaction intermediates. An excitation spectrum of the mixture in the stopped-flow instrument immediately after the reaction paralleled the absorbance spectrum of reduced enzyme obtained independently, confirming that the reduced enzyme was indeed the fluorescent species (data not shown). To our knowledge, only one other flavoprotein—lactate monooxygenase—has been reported to be more fluorescent in the reduced state than in the oxidized state (*28*).

The reduction with [$^2H_2$]-PAAP also had three phases, with lower observed rate constants for the first two steps, with values for the observed rate constants of 140 and 7.8 s^{-1} at saturating deuterated substrate concentrations for the first and second phases. A concentration of 0.32 mM PAAP produced a value of the first observed rate constant equal to half the saturated maximum, which is an isotope effect of 5.5 on this parameter. The observed rate constant of the last phase was not affected by the isotopic substitution (Table 2), in accord

Table 2: Kinetic Parameters Obtained from Simulations for the Reductive Half-Reaction of Amadoriase with PAAP[a]

		(s^{-1})				
substrate	k_1 ($M^{-1}s^{-1}$)	k_{-1}	k_2	k_{-2}	k_3	k_4
[$^1H_2$]-PAAP[b]	3.69×10^6	1740	476	12.3	23.4	3.3
[$^2H_2$]-PAAP[c]	3.69×10^6	1740	44.8	10.9	23.4	3.3

[a] All experiments were performed at pH 7.9, 4 °C. Varying the rate constants by more than ± 10% yielded simulations that deviated unacceptably from the data, as judged by visual inspection. [b] The values for [$^1H_2$]-PAAP were obtained by matching simulated reaction traces to experimental data. [c] The values for [$^2H_2$]-PAAP were obtained by only varying k_2 and k_{-2} in simulations.

with the hypothesis that the third observed step represents product release.

$$E_{ox} + S \underset{k_{-1}}{\overset{k_1}{\rightleftharpoons}} E_{ox}{\sim}S \underset{k_{-2}}{\overset{k_2}{\rightleftharpoons}} E_{red}{\sim}I \xrightarrow{k_3} E_{red}{\sim}P \overset{S \quad P}{\underset{k_4}{\rightleftharpoons}} E_{red}{\sim}S \quad (3)$$

Equation 3 represents the working model used to analyze the kinetic data, where E_{ox} represents the oxidized enzyme, E_{red} represents the reduced enzyme, S represents the active isomer of the substrate (see section below), I represents an intermediate, and P represents the product. Because the scheme has a sequence of reversible reactions, an exact solution to the differential equations governing the kinetics is not possible. As a first approximation, the concentration dependence of the observed rate constant for the first phase was analyzed according to the rapid equilibrium formalism of Strickland et al. (*16*), giving a flavin reduction rate constant of 594 s^{-1} (k_2) and a reverse reaction rate constant of 58 s^{-1} (k_{-2}). However, if the initial binding of PAAP were truly a rapid equilibrium process, the apparent K_d values should have been identical for the protio and deutero substrates; instead, a 5.5-fold isotope effect was observed. This suggested that the rapid equilibrium condition was not obeyed for PAAP binding, i.e., k_{-1} was not much larger than k_2. This has been noted in other cases for amine oxidation by flavoenzymes (*19*−*22*). Because the rapid equilibrium approximation was deemed invalid, the values of the rate constants were adjusted to satisfy the expressions derived by applying the steady-state approximation to the intermediates in eq 3 and assuming an arbitrary value of $\sim 10^5$ M^{-1} s^{-1} for k_1. These values were then used as initial estimates for globally fitting the differential equations describing eq 3 using a data set consisting of absorbance traces obtained at 453 nm, with the total concentration of PAAP varying from 125 μM to 25 mM. (As described in the section below, the active isomer of PAAP is 75% of the total.) The values obtained by this procedure are listed in Table 2 and were used to calculate the traces in Figure 2B. A value of 476 s^{-1} was obtained for the rate constant for the conversion of the Michaelis complex to the first intermediate. This intermediate converted to the reduced enzyme−product complex with a rate constant of 23.4 s^{-1}. These values were then used as starting estimates for simulating traces obtained in the reaction of [$^2H_2$]-PAAP. It was possible to satisfactorily simulate the [$^1H_2$]-PAAP data by changing only the rate constants governing the interconversion of E_{ox}∼S and E_{red}∼I; a kinetic isotope effect of 11 was calculated for the formation of E_{red}∼I (Table 2).

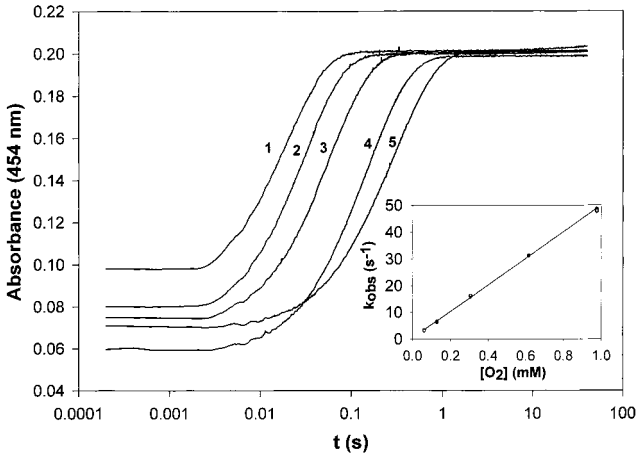

FIGURE 5: Time course of anaerobic oxidation of reduced amadoriase followed at 453 nm in a stopped-flow instrument. Amadoriase was reduced by PAAP anaerobically and mixed with buffers containing different concentrations of O_2. The experiments were made in 10 mM Tris HCl buffer, pH 7.9, at 4 °C. O_2 concentrations for curves 1−5 are 0.975, 0.61, 0.32, 0.128, and 0.061 mM. In the inset, the plot of [O_2] versus observed rate constants fitted from the reaction traces. Values of [O_2] are those after mixing.

The spectra of the species in eq 3 were calculated by deconvoluting spectra obtained in the diode-array experiments using [$^1H_2$]-PAAP as substrate. The spectra of the starting oxidized enzyme and the final reduced enzyme were considered to be known, and the spectrum of the free reduced enzyme was omitted from the calculation because this species never accumulated in reaction simulations. Three unknown spectra—those of E_{ox}∼S, E_{red}∼I, and E_{red}∼P—remained to be calculated. The concentrations of all species in eq 3 at 2, 6, and 102 ms were obtained by solving numerically the differential equations describing the reaction sequence. The absorbance at each time obeys Beer's law, giving three simultaneous equations in three unknowns, which was solved to produce the spectra shown in Figure 4. The spectrum of E_{ox}∼S shows a decrease in extinction and a slight shift to the peak absorbance of the oxidized flavin. The spectrum of E_{red}∼P has broad absorbance in the 450−550 nm region due to a reduced flavin-product charge-transfer transition. The broad absorbance spectrum of E_{red}∼I is not easily understood but appears to be a mixture of several species, with some characteristics of reduced flavin, a C4a adduct (peak at 400 nm), and oxidized flavin.

Oxidative Half-Reaction. At 4 °C, PAAP-reduced anaerobic enzyme was mixed with Tris buffer, pH 7.9, containing different oxygen concentrations. The oxidation of the enzyme by oxygen exhibited a single phase over a wide range of oxygen concentrations (0.06−0.975 mM). The reaction was followed by measuring the increase in flavin absorption at 453 nm. Analysis of the time courses based on eq 2 described in the Experimental Procedures gave a single first-order rate constant, k_{obs}. The plot of k_{obs} versus [O_2] was linear (Figure 5, inset), giving a bimolecular rate constant of 4.9×10^4 M^{-1} s^{-1}. The strictly second-order reaction of the enzyme with O_2 over all attainable concentrations is typical for flavin oxidases and oxygenases (*26*).

As described above, product release from the reduced enzyme is too slow to be catalytically relevant. Instead, O_2 must react with the reduced enzyme−product complex. We examined this directly in double-mixing stopped-flow experi-

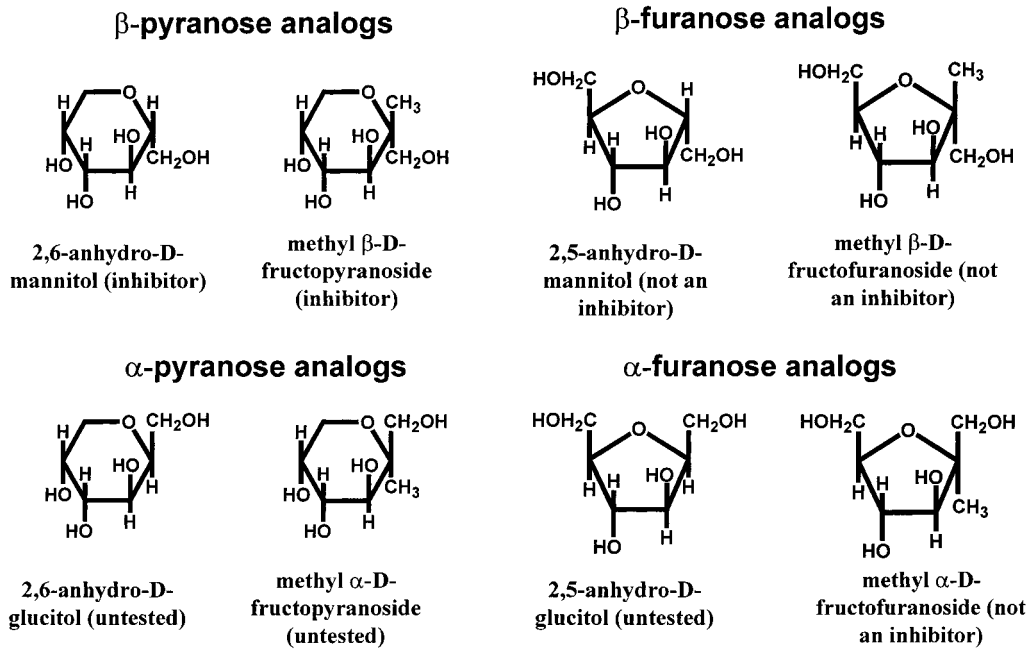

FIGURE 6: Structures of the substrate analogues used in inhibition study.

ments by first mixing anaerobic oxidized enzyme with an anaerobic solution containing one equivalent of PAAP. The enzyme was allowed to become reduced (390 ms), and, before the product dissociated to a significant extent, the reduced enzyme−product complex was mixed with buffer solutions containing various amounts of oxygen. The observed rate constant for the oxidation of the enzyme was linear, giving a bimolecular rate constant of 3.6×10^4 M^{-1} s^{-1}. Thus, the presence of the product barely alters the reaction rate of O_2, confirming that the reduced enzyme−product complex is a catalytically competent intermediate.

Inhibition Studies with Substrate Analogues. A solution of ketose at equilibrium contains a mixture of α- and *β*-pyranoses and a mixture of α- and *β*-furanoses in addition to the acyclic form. Generally, the furanose anomers are favored kinetically, whereas pyranose anomers are favored thermodynamically and thus are more abundant under equilibrium conditions (*23*). D-Fructose at room temperature is 69.6% *β*-pyranose, 3% α-pyranose, 21.1% *β*-furanose, 5.7% α-furanose, and 0.5% open chain forms, whereas Amadori products at room temperature show approximately 61% *β*-pyranose, 6% α-pyranose, 15% *β*-furanose, 16% α-furanose, and 2% keto forms (*23*). Reducing the carbonyl to a hydroxyl on the Amadori product will prevent it from forming a cyclic hemiketal. The borohydride-reduced Amadori adduct, 1-deoxy-glucitoyl propylamine, is neither a substrate nor an inhibitor (9), suggesting that the enzyme does not recognize the acyclic form of the substrate. It was also discovered that fructose, part of the substrate structure, serves as an inhibitor of the enzyme. Since fructose also consists of pyranose and furanose forms in solution, compounds that are analogues of either of those ring forms but are locked chemically into a given configuration were tested as inhibitors. The compounds used and the results obtained are shown in the Figure 6. From this inhibition study, we found that none of the furanose analogues is an inhibitor of amadoriase, while the *β*-pyranose analogues 1,5-anhydro-D-mannitol and methyl *β*-fructopyranoside (Figure 7) are

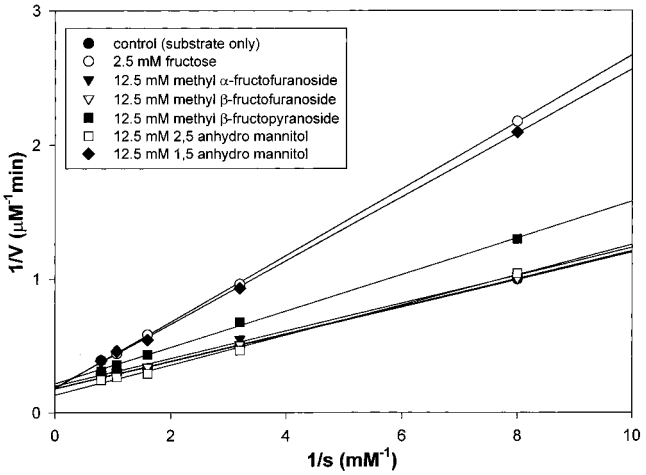

FIGURE 7: Inhibition of amadoriase activity by substrate analogues. Double-reciprocal plot of the relationship between substrate concentrations and the rates of H_2O_2 formation. Experiments were conducted at room temperature in 10 mM HEPES buffer, pH 8.0 (see Experimental Procedures).

inhibitors but weaker than fructose. We did not test any α-pyranose analogues due to their lack of availability.

Direct Kinetic Determination of Substrate Specificity. Besides inhibition studies using fructose analogues, kinetic measurements were also used to determine which isomer of the substrate is recognized by amadoriase. To perform such a study, an excess of enzyme over substrate was used in anaerobic mixing experiments. The reactive anomer of the substrate should react rapidly, while the other isomers will first need to isomerize, causing the rate of reduction after the initial fast reaction to be determined by the rate of the resupply of the reactive form of the substrate by the remaining substrate pool.

Various concentrations of amadoriase (∼70−110 *μ*M before mixing) were mixed with 50 *μ*M PAAP (before mixing) in the stopped-flow apparatus under anaerobic condition at 4 °C. Reactions were followed at 453 and 550

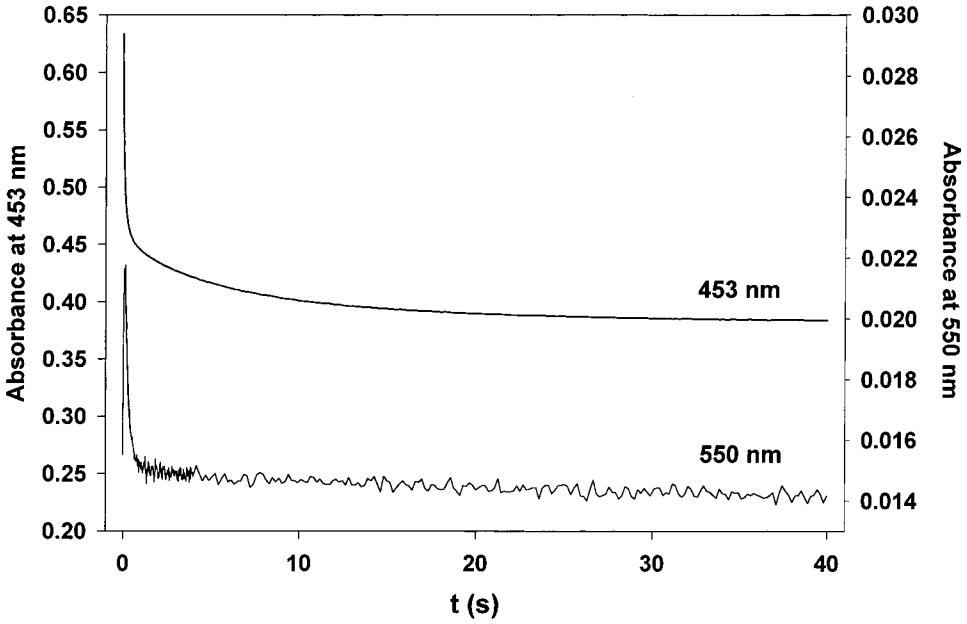

FIGURE 8: Kinetic determination of the reactive configuration of PAAP. An excess of amadoriase (70−110 μM) was mixed with 50 μM [$^1H_2$]-PAAP. The experiments were in 10 mM Tris buffer, pH 7.9, at 4 °C, and the results are summarized in Table 3.

Table 3: Kinetic Constants for the Reaction of Excess Amadoriase with PAAP, at pH 7.9, 4 °C[a]

enzyme conc (μM)	109	100	74.6
A_1	0.10	0.11	0.12
k_1 (s^{-1})	31.3	26.2	18.7
A_2	0.08	0.07	0.06
k_2 (s^{-1})	6.4	4.6	3.4
A_3	0.06	0.07	0.07
k_3 (s^{-1})	0.12	0.15	0.16

[a] Substrate concentration is 50 μM after Mixing. *k* is the observed rate constant of each phase and A is the amplitude

nm for 40 s, until the absorbance was constant (Figure 8). Analysis of the traces gave two relatively fast phases followed by a very slow third phase (Table 3). Data at 550 nm showed formation and decay of an intermediate within 1 s. The first two phases represent the binding of the substrate, reduction of the flavin, and product release. (At the concentrations of reactants used here, the reactions are no longer resolved, as they were in the studies described above for the reductive half-reaction.) The third phase is much slower (~0.15 s^{-1}) than the product release step (3.5 s^{-1}) that we observed during the reductive half-reaction and occurs after the decay of the charge transfer complex (Figure 8). Thus, it is unlikely to be involved in any catalytic reactions. We attribute this phase to the spontaneous conversion of other isomers of the substrate into the one that is recognized by the enzyme. Table 3 lists the observed rate constants of three phases and their amplitudes using different enzyme concentrations. The rate of the last reaction was essentially independent of enzyme concentration, consistent with it being the substrate interconversion step. A comparison of the amplitudes of each phase reveals that approximately 75% of the substrate reacts in the fast initial reactions, whereas 25% of the substrate can only be oxidized after it spontaneously isomerizes. On the basis of the composition of the equilibrium mixture of Amadori products in solution (*23*), we conclude that the β-pyranose isomer, the most abundant configuration in the solution, is the form of the substrate that is recognized by the enzyme, which is consistent with the results from inhibition studies.

DISCUSSION

Our results suggest that amadoriase binds the β-pyranose isomer of PAAP. This conclusion is based on the inhibition data, which indicated that a pyranose ring is required for ligand binding, and by our kinetic data on anomer preference. We found that 75% of PAAP reduced the enzyme rapidly, while 25% of PAAP slowly isomerized before reducing the enzyme. The apparent rate constant of ~0.15 s^{-1} at 4° for the replenishment of the β-pyranose isomer of PAAP is close to what might be expected given the values measured for other sugars at 25°, e.g., 8.1 s^{-1} for fructose-1,6-bis phosphate (*29*). The amount of β-pyranose isomer of the Amadori product has previously been determined by NMR as 61%, in rough agreement with our kinetic estimate. We attribute the small difference between the NMR determination and our kinetic result to the different conditions used in the two measurements, especially the temperature. If the difference in equilibrium positions is due to temperature effects alone, then a van't Hoff analysis gives an estimate of 1.6 kcal mol^{-1} as the enthalpy difference between the β-pyranose anomer and the ensemble of the other isomers.

Three reactions were observed after the binding of PAAP to amadoriase. The last reaction represents product dissociation, while the two preceding reactions result in flavin reduction. The mechanism of flavin reduction by PAAP, and the identity of the species we have designated E_{red}~I, are not immediately apparent. The calculated absorbance spectrum of E_{red}~I does not correspond to any known flavin derivative but appears to be due to the presence of several species (Figure 4). The broad absorbance from 345 to 385 nm is suggestive of reduced flavin or an N5 adduct. The peak at 400 nm suggests either anionic semiquinone or a C4a adduct, but the absorbance at 380 nm is too low as compared to the absorbance at 400 nm for there to be anionic semiquinone, so the possibility of a flavin radical may be

Scheme 1: Possible Mechanisms for PAAP Oxidation by Amadoriase I

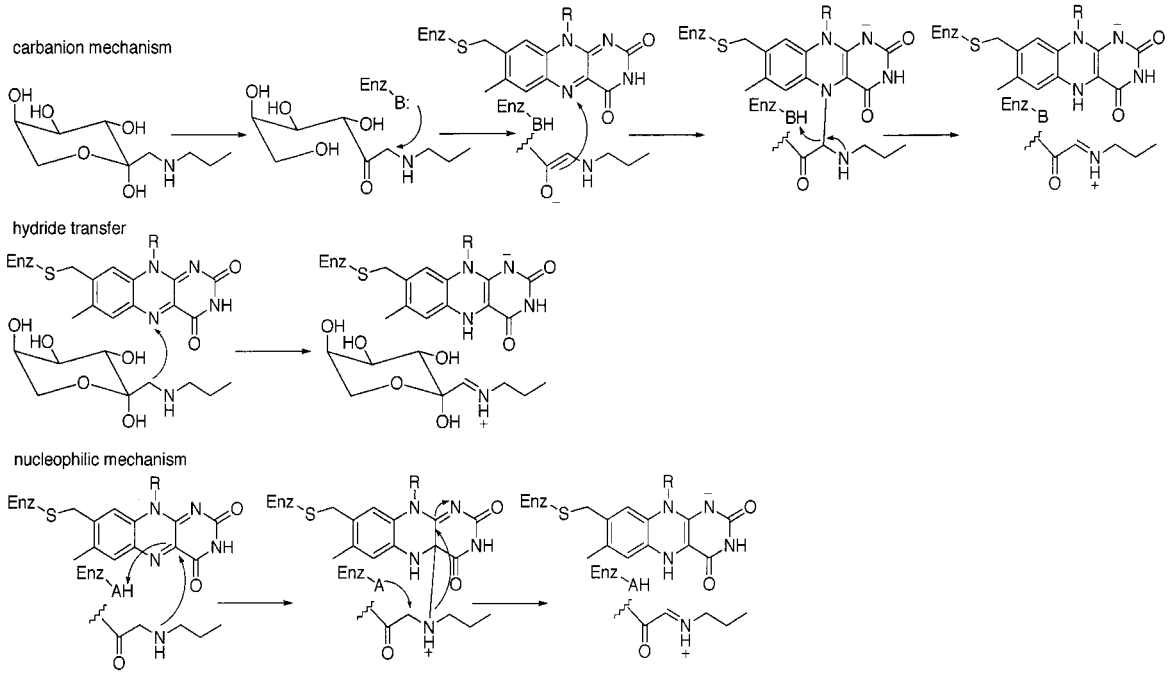

eliminated. The absorbance shoulder at 456 nm suggests that oxidized flavin could be contributing to the spectrum. The complex spectrum obtained for E_{red}∼I cannot yet be explained, but three possibilities are suggested here. (i) Perhaps the species that we have denoted as E_{red}∼I is actually a rapidly equilibrating mixture of species, so that kinetically it forms and reacts as a single species but has the spectral properties of the components. A number of chemical intermediates have been invoked in reactions that form reduced flavin, but these intermediates are rarely (if ever) thought to be observed spectrally. It is conceivable that I represents such a redox intermediate. (ii) Alternatively, the unusual spectrum of E_{red}∼I could be due to an unusual interaction between the reduced flavin and the initial reaction product, which is presumably the iminium cation. In this scenario, any intermediates on the pathway to reduced flavin (if they occur) would be kinetically invisible, and any of the large number of flavin reduction mechanisms that have been proposed would be consistent with our results. (iii) Last, it should not be forgotten that the spectra in Figure 4 have been calculated based on the scheme in eq 3. If this mechanism is not correct, then the resulting spectra will also be incorrect.

The chemical mechanism of the reduction of flavins by amines and alcohols has been the subject of intense research for several decades (*13*, *33*, *38*). Several mechanisms for the reduction of flavins by amines have been proposed (Scheme 1). The amino acid oxidases had been thought to oxidize amino acids to imino acids by first deprotonating the substrate with an active site base, forming a carbanion-equivalent as an intermediate (*37*). The electron-rich nucleophilic intermediate would then rapidly reduce the flavin, either by forming a covalent adduct between the amino acid and N5 of the flavin followed by elimination, or by rapid single electron transfers. A nucleophilic mechanism has also been proposed where the amine of the substrate attacks C4a of the flavin, followed by base catalyzed oxidative elimination. An alternative to this mechanism that has gained favor recently is a hydride transfer mechanism, in which the flavin is reduced without intermediates (*22*). Other mechanisms for flavin reduction by amines have been proposed for monoamine oxidase (*32*). It should be stressed that in all these proposed mechanisms, the formation of the intermediates (if present) is assumed to be rate-determining, accounting for the fact that none of the proposed intermediates have ever been directly observed. Any of these mechanisms could be operational in amadoriase if E_{red}∼I represents the enzyme after flavin reduction, as in scenario (ii) above. On the other hand, it is conceivable that scenario (i) applies, and E_{red}∼I is one of the intermediates described above, excluding the hydride transfer mechanism. Carbanionic intermediates are generally unstable species, and the pyranose form of PAAP offers no inherent stabilization. The keto form of PAAP could stabilize some of the intermediates described above. A carbonyl group would acidify the protons on the adjacent carbon, assisting the carbanion mechanism through the formation of an enolate intermediate. However, our data indicate that it is the pyranose form of the substrate that is recognized by the enzyme. This does not exclude an enzyme-catalyzed ring-opening reaction, generating the keto group at the active site prior to redox chemistry. If this were the case, then the lack of inhibition by the acyclic substrate analogue would imply that the protein has a strict requirement for the cyclic conformation to bind the sugar.

If scenario (i) above were operational, then E_{red}∼I would represent one of the reduction intermediates described above or a rapidly equilibrating mixture of some of these species. It must be remembered that E_{red}∼I does not have the spectrum of the anionic or neutral flavin semiquinone, nor would a single electron-transfer reaction have a large deuterium isotope effect associated with it, eliminating mechanisms that would form semiquinone. This leaves the possibility of either a PAAP-flavin C4a adduct or a carbanion mechanism if an enzymatic base initiates the redox chemistry. In either case, the unusual absorbance spectrum calculated for E_{red}∼I would be at least partially due to interactions

Scheme 2: Proposed Kinetic Mechanism for the Catalytic Cycle of Amadoriase I

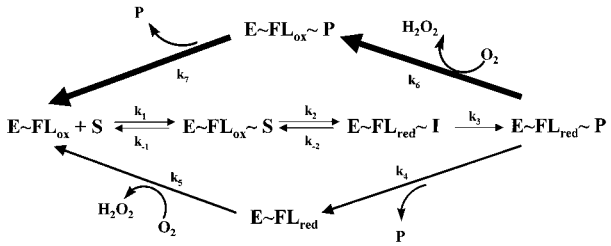

between the intermediate and the flavin. Enolate−flavin interactions are imaginable in the case of a carbanion mechanism, as are amine−flavin interactions in the case of nucleophilic mechanism. In either case, the reduced enzyme−product complex would be formed upon complete reduction of the flavin.

If scenario (ii) above is operational, then the first phase would then represent the reduction of the flavin by a hydride equivalent—by an undetermined mechanism—from C1 of PAAP, forming an iminium ion as the immediate product. The conversion of E_{red}~I to E_{red}~P would then represent either the deprotonation of the iminium cation to the imine, or the hydrolysis of the iminium species to the glucosone product while it is still bound to the enzyme. The unusual spectrum calculated for E_{red}~I would then be due to unusual interactions between the reduced isoalloxazine and the iminium cation.

The rate constant for product dissociation (3.5 s^{-1}) was lower than the overall turnover number of the enzyme (14.4 s^{-1}), indicating that molecular oxygen reacts with the reduced enzyme−product complex rather than the free reduced enzyme. Our double-mixing experiments demonstrated that this was a catalytically relevant pathway, since the reaction of the reduced enzyme−product complex with O_2 occurred with nearly the same rate constant as the reaction of the free enzyme. We propose the total kinetic mechanism in Scheme 2, where thicker arrows represent the actual pathway followed during turnover. Using the net rate constant method (*31*), an expression for k_{cat} (eq 2) was derived for the catalytic pathway in Scheme 2.

$$k_{cat} = \left[\frac{k_{-2} + k_3}{k_2 k_3} + \frac{1}{k_3} + \frac{1}{k_7}\right]^{-1} \quad (4)$$

The value of k_{cat} is determined by the rate constants for the reaction of the Michaelis complex to form the first intermediate, the rate constant for the conversion of this intermediate to the charge transfer complex, and the rate constant for product release. From our experiments, we have directly estimated values for k_2, k_{-2}, and k_3, but product release from the oxidized enzyme (k_7) was not directly observable. To obtain the observed value of 14.4 s^{-1} for k_{cat}, a value of 42.6 s^{-1} must be used for k_7, the rate constant for product release. Thus, the overall turnover number at pH 7.9, 4° appears to be determined by two steps: the conversion of the first intermediate into the reduced enzyme−product charge-transfer complex and the release of product from the oxidized enzyme. In the case of the dideuterated substrate, the reduction of the flavin (k_2) becomes 11-fold slower, causing this step to also become partially rate-determining. However, the values for the rate constants obtained from the reductive half reaction using [$^2H_2$]-PAAP, combined with the value for k_7 estimated for [$^1H_2$]-PAAP, predict a value of k_{cat} that is 2-fold higher than the value actually measured for [$^2H_2$]-PAAP, suggesting either a large degree of error in our estimate or a more complex kinetic scheme.

Amadoriase goes through an ordered ternary complex in turnover, despite the constant k_{cat}/K_m for O_2 at different levels of PAAP that is normally characteristic of a ping-pong kinetic mechanism. Such apparently contradictory observations have been made in the past with other flavoprotein oxidases (*10*) and have been explained by a thermodynamically irreversible step prior to the reaction of O_2. The two electron reduction potential of amadoriase is relatively high (−2 mV), making this a very plausible explanation.

ACKNOWLEDGMENT

We thank Professors David P. Ballou and Vincent Massey (University of Michigan) for allowing us to use their facilities.

REFERENCES

1. Takahashi, M., Pischetsrieder, M., and Monnier, V. M. (1997) *J. Biol. Chem. 272*, 3437−3443.
2. Grandhee, S. K., and Monnier, V. M. (1991) *J. Biol. Chem. 266*, 11649−11653.
3. Dyer, D. G., Blackledge, J. A., Thorpe, S. R., and Baynes, J. W. (1991) *J. Biol. Chem. 266*, 11654−11660.
4. Ahmed, M. U., Thorpe, S. R., and Baynes, J. W. (1986) *J. Biol. Chem. 261*, 4889−4894.
5. Sell, D. R., Lapolla, A., Odetti, P., Fogarty, J., and Monnier, V. M. (1992) *Diabetes 41*, 1286−1292.
6. McCance, D. R., Dyer, D. G., Dunn, J. A., Bailie, K. E., Thorpe, S. R., Baynes, J. W., and Lyons, T. J. (1993) *J. Clin. Invest. 91*, 2470−2478.
7. Beisswenger, P. J., Moore, L. L., Brinck-Johnsen, T., and Curphey, T. J. (1993) *J. Clin. Invest. 92*, 212−217.
8. Baynes, J. W., and Monnier, V. M. (1989) *Prog. Clin. Biol. Res. 304*, 1−410.
9. Wu. X., Takahashi, M., Chen, S. G.; Monnier. V. M. (2000) *Biochemistry 39*, 1515−1521.
10. Pollegioni, L., Fukui, K., and Massey, V. (1994) *J. Biol. Chem. 269*, 31666−31673.
11. Massey, V. (1991) in *Flavins and Flavioproteins* 1990 (Curti, B., Ronchi, S., and Zanetti, G., Eds.) pp 59−66, Walter de Gruyter, New York.
12. Gibson, Q. H., Swoboda, B. E. P., Massey, V. (1964) *J. Biol. Chem. 239*, 3927−3934.
13. Palfey, B. A., and Massey, V. in *Comprehensive Biological Catalysis* (1998) (Sinnott, M., Ed.) Volume III, pp 83−154, Academic Press Limited, New York.
14. Clark, W. M. (1960*) Oxidation−Reduction Potentials of Organic Compounds*, pp 184−203, Williams and Wilkins, New York.
15. Minnaert, K. (1965*) Biochim. Biophys. Acta 110*, 42−56.
16. Strickland, S., Pamler, G., Massey, V. (1975) *J. Biol. Chem. 250*, 4048−4052.
17. Massey, V., and Gibson, Q. H. (1964) *Fed. Proc. U.S.A. 23*, 18−29.
18. Schopfer, L. M., and Massey, V. (1988) *Biochemistry 27*, 6599−6611.
19. Port, D. J. T., Voet, J. G., and Bright H. J. (1977) *J. Biol. Chem. 252*, 4464−4473.
20. Pollegioni, L., Langkau, B., Tischer, W., Ghisla, S., and Pilone, M. S. (1993) *J. Biol. Chem. 268*, 13850−13857.
21. Fitzpatick, P. F., and Massey, V. (1982) *J. Biol. Chem. 257*, 12916−12923.
22. Pollegion, L., Blodig, W., and Ghisla, S. (1997) *J. Biol. Chem. 272*, 4924−4934.

23. Yaylayan, V. A., and Huyghues-Despointes, A. (1994) *Crit. Rev. Food Sci. Nutr. 34*, 321−369.
24. Myszka, D. G., and Morton, T. A. (1998) *Trends Biochem. Sci. 23*, 149−150.
25. Patil, P. V., and Ballou, D. P. (2000) *Anal. Biochem. 286*, 187−192.
26. Massey, V. (1994) *J. Biol. Chem. 269*, 22459−22462.
27. Massey, V., Stankovich, M., and Hemmerich, P. (1978) *Biochemistry 17*, 1−8.
28. Ghisla, S., Massey, V., Lhoste, J.-M., and Mayhew, S. G. (1979) *Eur. J. Biochem. 101*, 13−21.
29. Benkovic, S. J. (1979) *Methods Enzymol. 63*, 370−379.
30. Schopfer, L. M., Massey, V., and Nishino, T. (1988) *J. Biol. Chem. 263*, 13528−13538.
31. Cleland, W. W. (1975) *Biochemistry 14*, 3220−3224.
32. Edmondson, D. E. (1995) *Xenobiotica 25*, 735−753.
33. Silverman, R. B., Hoffman, S. J., and Catus, W. B. (1980) *J. Am. Chem. Soc. 102*, 7126−7128.
34. Duker, J. M., and Serianni, A. S. (1993) *Carbohydr. Res. 249*, 281−303.
35. Walker, T. E., Unkefer, C. J., and Ehler, D. S. (1988) *J. Carbohydr. Chem. 7*, 115−132.
36. Bethell, G. S., and Ferrier, R. J. (1973) *Carbohydr. Res. 31*, 69−80.
37. Walsh, C. T., Schonbrunn, A., and Abeles, R. H. (1971) *J. Biol. Chem. 246*, 6855−6866.
38. Fitzpatrick, P. F. (2001) *Acc. Chem. Res. 40*, 5352−5367.

BI011244E